Journal of proteome research

TECHNICAL NOTE

pubs.acs.org/jpr

Identification and Quantification of DNA Repair Proteins by Liquid Chromatography/Isotope-Dilution Tandem Mass Spectrometry Using Their Fully ^{15}N-Labeled Analogues as Internal Standards

Miral Dizdaroglu,* Prasad T. Reddy, and Pawel Jaruga

Biochemical Science Division, National Institute of Standards and Technology, Gaithersburg, Maryland 20899-8311, United States

Supporting Information

ABSTRACT: Oxidatively induced DNA damage is implicated in disease, unless it is repaired by DNA repair. Defects in DNA repair capacity may be a risk factor for various disease processes. Thus, DNA repair proteins may be used as early detection and therapeutic biomarkers in cancer and other diseases. For this purpose, the measurement of the expression level of these proteins in vivo will be necessary. We applied liquid chromatography/isotope-dilution tandem mass spectrometry (LC−MS/MS) for the identification and quantification of DNA repair proteins human 8-hydroxyguanine-DNA glycosylase (hOGG1) and *Escherichia coli* formamidopyrimidine DNA glycosylase (Fpg), which are involved in base-excision repair of oxidatively induced DNA damage. We overproduced and purified ^{15}N-labeled analogues of these proteins to be used as suitable internal standards to ensure the accuracy of quantification. Unlabeled and ^{15}N-labeled proteins were digested with trypsin and analyzed by LC−MS/MS. Numerous tryptic peptides of both proteins were identified on the basis of their full-scan mass spectra. These peptides matched the theoretical peptide fragments expected from trypsin digestion and provided statistically significant protein scores that would unequivocally identify these proteins. We also recorded the product ion spectra of the tryptic peptides and defined the characteristic product ions. Mixtures of the analyte proteins and their ^{15}N-labeled analogues were analyzed by selected-reaction monitoring on the basis of product ions. The results obtained suggest that the methodology developed would be highly suitable for the positive identification and accurate quantification of DNA repair proteins in vivo as potential biomarkers for cancer and other diseases.

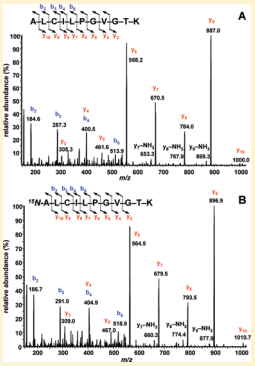

KEYWORDS: cancer biomarkers, DNA damage, DNA repair proteins, mass spectrometry, OGG1

Oxidatively induced DNA damage has been implicated as a major factor in carcinogenesis and aging.[1,2] Various in vivo pathways exist to repair DNA damage. DNA repair is essential for the maintenance of genomic stability and plays a major role in prevention of disease processes.[2,3] Defects in DNA repair constitute a risk factor for cancer.[4−13] Germline mutations and polymorphisms in DNA repair genes are associated with genomic instability and predisposition to cancer.[3,8,11,13,14] There is evidence for a connection between several types of cancer and the polymorphic forms of the repair enzyme 8-hydroxyguanine-DNA glycosylase (OGG1).[8,15−25] This enzyme is involved in the base excision repair (BER) of oxidatively damaged DNA, specifically removing 2,6-diamino-4-hydroxy-5-formamidopyrimidine (FapyGua) and 8-hydroxyguanine (8-OH-Gua).[26−28] Defects in expression of DNA repair proteins may lead to therapy resistance and affect overall survival in cancer patients.[11,13,29−31] Low human OGG1 (hOGG1) activity has been shown to be a risk factor in lung cancer and several types of head and neck cancers.[32−37] Furthermore, DNA-damaging agents decrease expression levels of DNA repair proteins in human cells, possibly increasing health risk.[38] On the other hand, measurement of *ogg1* mRNA expression in a large number of human lung cancer and normal cell lines revealed overexpression in most cancer cell lines relative to controls.[39] Cancer cell lines with increased *ogg1* mRNA expression exhibited normal repair activity for the excision of 8-OH-Gua, whereas those with low *ogg1* mRNA expression accumulated greater levels of 8-OH-Gua, indicating that the expression of the gene relates to the amount of 8-OH-Gua excision. A more recent study also showed increased *ogg1* mRNA expression and 8-OH-Gua excision rate in colorectal carcinoma patients.[40] Increased levels of DNA repair proteins in cancerous tissues may adversely affect cancer therapy and thus patient survival.

In the present work, we aimed to develop methodologies using mass spectrometry with isotope-dilution for the positive identification and accurate quantification of DNA repair proteins. As examples, we chose hOGG1 and *Escherichia coli* formamidopyrimidine DNA glycosylase (Fpg). We applied liquid chromatography/tandem mass spectrometry (LC−MS/MS) with isotope-dilution using fully ^{15}N-labeled analogues of hOGG1 and Fpg as internal standards.

MATERIALS AND METHODS

Reagents

Trypsin, endorphin, acetonitrile (HPLC-grade), and water (HPLC-grade) for analysis by LC−MS/MS were purchased from Sigma (St. Louis, MO). Water purified through a Milli-Q

Received: April 11, 2011
Published: May 30, 2011

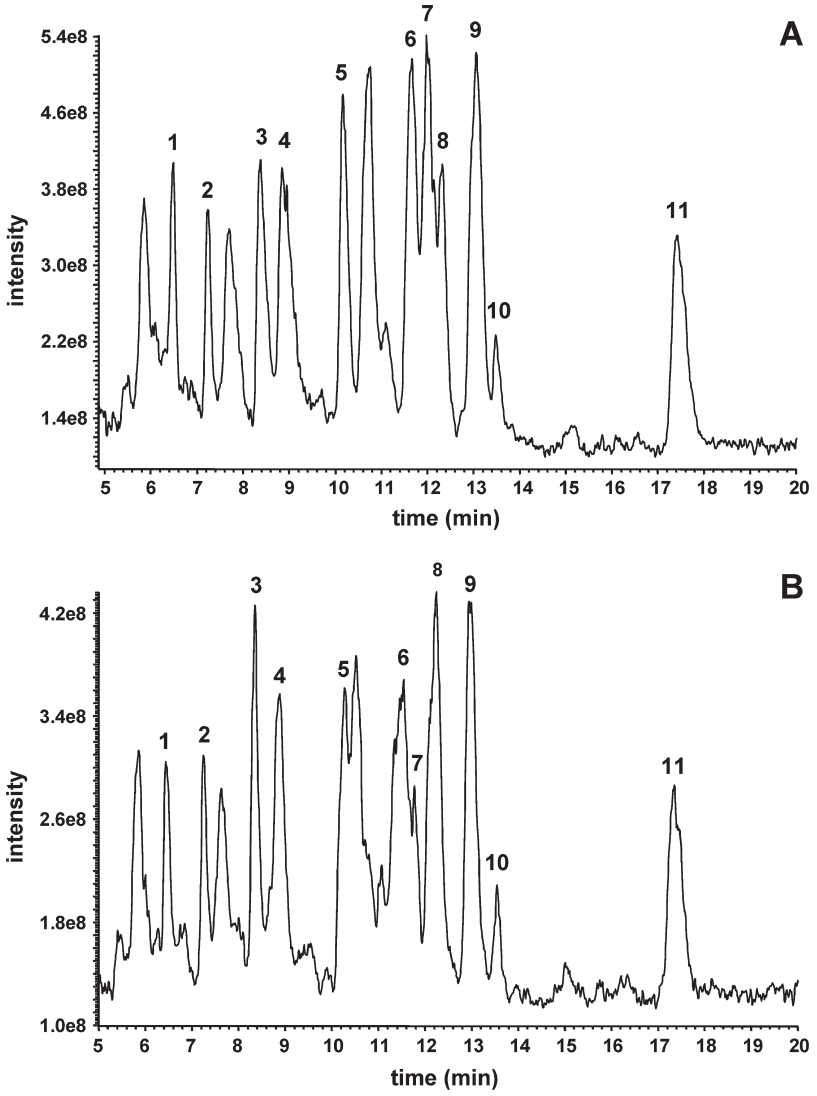

Figure 1. TIC profiles of tryptic digests of (A) hOGG1 and (B) ^{15}N-labeled hOGG1. Identities of the peaks are given in Table 1.

system (Millipore, Bedford, MA) was used for all other applications. Biomax5 ultrafiltration membranes (5 kDa molecular mass cutoff) were from Millipore (Bedford, MA).

Hydrolysis with Trypsin

An aliquot of 120 μg of hOGG1 or Fpg was incubated with 2.4 μg of trypsin in 600 μL of Tris buffer (30 mM, pH 7.5) at 37 °C for 24 h. The sample was heated at 95 °C for 10 min to inactivate trypsin and then filtered using ultrafiltration membranes (5 kDa molecular mass cutoff).

Instrumentation and Analysis

LC−MS/MS analyses were performed using a Thermo-Scientific Accela high speed LC system coupled to a Thermo-Scientific Finnigan TSQ Quantum Ultra AM triple quadrupole MS/MS system with an installed heated electrospray-ionization (HESI) source. Samples (2−40 μL injections, no waste mode) were analyzed using a Zorbax Eclipse XDB-C18 narrow-bore LC column (2.1 mm × 150 mm, 3.5 μm particle size) (Agilent Technologies, Wilmington, DE) with an attached Agilent Eclipse XDB-C8 guard column (2.1 mm × 12.5 mm, 5 μm particle size). In all instances, the autosampler and column temperature were kept at 15 and 30 °C, respectively. Mobile phases A and B were water and acetonitrile, respectively. A gradient analysis of 2% (v/v) of B/min starting from 96%A/4%B (v/v) was used. After 21 min, B was increased to 90% in 0.1 min and kept at this level for 14 min and then another 30 min at 4% to equilibrate the column. The flow rate was 250 μL/min, and the total analysis time was 65 min.

Automated mass calibration of the MS/MS system in positive ion mode was performed by infusing a solution of polytyrosine-1,3,6 and monitoring the specified protonated MH^+ monomer (m/z 182), trimer (m/z 508), and hexamer (m/z 997) ions. MS/MS operating parameters were fine-tuned by simultaneously infusing a solution of endorphin (0.03 mM) in water via syringe pump and the LC mobile phase via the Accela LC pump through a T-connection directly into the HESI source probe. The following MS/MS parameters were used for all measurements: spray voltage = 3.5 kV; tube lens offsets = 87 V for Q1 and Q3; vaporizer temperature = 250 °C; capillary temperature = 340 °C; sheath gas (nitrogen) pressure = 60 (arbitrary units); auxiliary gas (nitrogen) pressure = 35 (arbitrary units); collision gas (argon) pressure = 6.67 × 10^{-5} Pa (5 mTorr). The collision energy for each tryptic peptide was determined experimentally

dx.doi.org/10.1021/pr200269j |J. Proteome Res. 2011, 10, 3802–3813

by analyzing each peptide at different energy units and found to vary between 20 and 32 V. Full-scan spectra (Q1-spectra) of tryptic peptides were recorded in the positive ion mode using the m/z range from 100 to 1500 Th under unit mass resolution Q1 = 0.7 and Q3 = 0.7 full width half-maximum (fwhm) with a scan time of 0.4 s. Product ion spectra (MS/MS spectra) of tryptic peptides were obtained under unit mass resolution Q1 = 0.9 and Q3 = 0.7 fwhm with a scan time of 0.4 s. Selected reaction monitoring (SRM) [also called multiple reaction monitoring (MRM)] was performed via positive ion mode under unit mass resolution Q1 = 1 and Q3 = 1 fwhm. The scan time and scan width were 0.01 s and m/z 4, respectively.

Table 1. Identification of the Peaks in Figure 1A and B[a]

		unlabeled peptide		^{15}N-labeled peptide	
peak	peptide	MH^+	$(M + 2H)^{2+}$	MH^+	$(M + 2H)^{2+}$
1	ITGMVER	805.4	403.2	815.4	408.2
2	YVSASAR	753.4	377.2	763.4	382.2
3	FQGVR	606.3	303.7	615.3	308.2
4	DYSWHPTTSQAK	1420.6	710.8	1437.6	719.3
5	LLR	401.3	201.1	407.3	204.1
6	ELGNFFR	882.4	441.5	893.4	447.2
7	ALLPR	569.4	285.2	577.4	289.2
8	LDLVLPSGQSFR	1331.7	666.4	1347.7	674.4
9	LGLGYR	678.5	339.7	687.5	344.2
10	LCQAFGPR	891.5	446.2	903.5	452.2
11	ALCILPGVGTK	1071.6	536.3	1083.6	542.3

[a] Sequences of the peptides and monoisotopic masses (Da) of their MH^+ and $(M + 2H)^{2+}$ ions.

RESULTS

The aim of this work was to develop assays to identify and quantify DNA repair proteins in vivo by mass spectrometric techniques. We chose two major DNA repair proteins, hOGG1 and *E.coli* Fpg, in our investigations and applied LC−MS/MS with isotope-dilution. For the measurement of a protein by mass spectrometry, an ideal internal standard would be its analogue labeled with stable isotopes such as ^{15}N, because the stable isotope-labeled protein would possess identical chemical and physical properties as the analyte protein and thus compensate

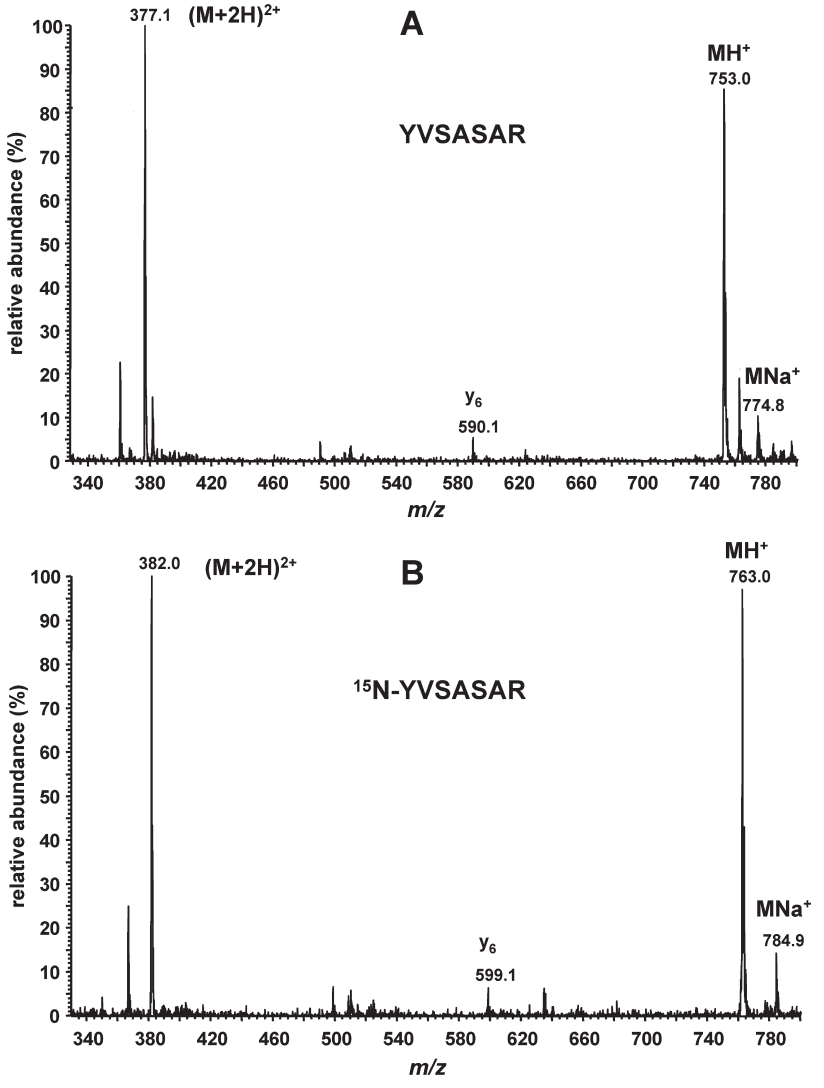

Figure 2. Full-scan mass spectra of (A) YVSASAR (peak 2 in Figure 1A) and (B) ^{15}N-YVSASAR (peak 2 in Figure 1B).

dx.doi.org/10.1021/pr200269j |J. Proteome Res. 2011, 10, 3802–3813

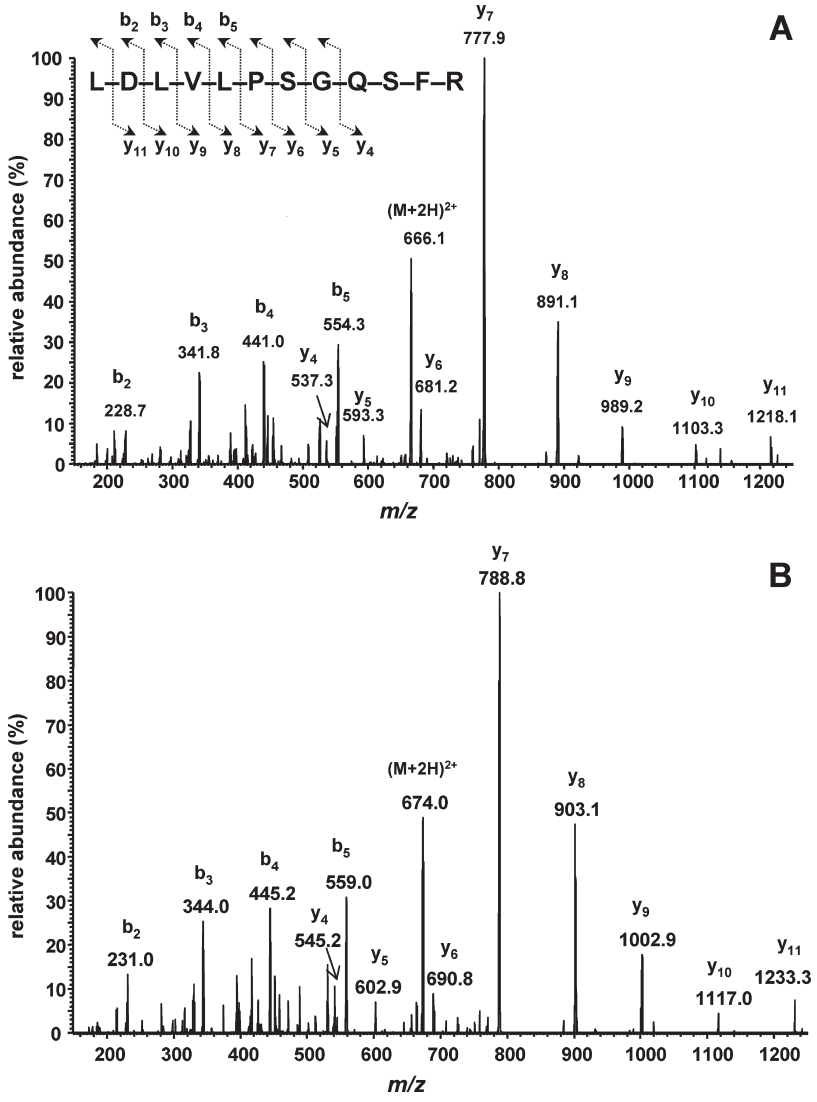

Figure 3. (A) MS/MS spectra of LDLVLPSGQSFR (peak 8 in Figure 1A) and (B) ^{15}N-LDLVLPSGQSFR (peak 8 in Figure 1B).

for eventual losses during analysis. We previously reported on the production, isolation, and characterization of the fully ^{15}N-labeled analogues of Fpg and hOGG1.[41] hOGG1 exists in various isoforms (http://www.uniprot.org/uniprot/O15527). Isoform 1A (α-hOGG1) with 345 amino acids is the most abundant form of this protein and differs from the second most abundant isoform, isoform 2A (*β*-hOGG1), by 79 amino acids.[42] α-hOGG1 and *β*-hOGG1 result from an alternative splicing after the transcription of the *hogg1* gene on chromosome 3p25 and are located to the nucleus and the mitochondrion, respectively.[43−45] These isoforms have an identical sequence up to 316 amino acids at the N-terminus; however, they exhibit a different sequence at the C-terminus.[45] As a result, the 30 theoretical tryptic peptides of both α-hOGG1 and *β*-hOGG1 that would result from trypsin digestion are identical.

In this work, we used α-hOGG1 (called hOGG1 from here on) and Fpg. These proteins and their ^{15}N-labeled analogues were subjected to digestion with trypsin, which hydrolyzes peptide bonds at the C-terminus sides of Lys (except when Pro is attached) and Arg.[46] The hydrolysates were analyzed by LC−MS/MS to separate the resulting tryptic peptides and to obtain their mass spectra for identification. hOGG1 has 345 amino acids and an average molecular mass of 38 782 Da. Theoretically, the trypsin digestion of hOGG1 yields 38 fragments, 6 of which are single amino acids: 3 arginines and 3 lysines. The lengths of the 32 peptides vary from 2 to 31 amino acids (http://au.expasy.org/tools/pi_tool.html). hOGG1 used in this work was His-tagged with a sequence GSSHHHHHHSSGLVPRGSHMEL, which replaces Met at the N-terminus of the protein, resulting in a molecular mass of 41 187.8 Da. The His-tag does not affect the masses of the tryptic peptides except for the first one at the N-terminus. Fpg contains 269 amino acids with an average molecular mass of 30 290 Da. Fpg yields 33 tryptic fragments including 3 single arginines and 3 single lysines. The tryptic peptides contain 2−28 amino acids.

Analysis of hOGG1

Figure 1A illustrates the total-ion-current (TIC) profile of the trypsin hydrolysate of hOGG1. The full-scan mass spectra of the compounds represented by the peaks in Figure 1A were recorded. On the basis of their mass spectra, we identified 11 tryptic peptides that matched the theoretical peptide fragments expected from trypsin digestion of hOGG1. The identities of the

dx.doi.org/10.1021/pr200269j |*J. Proteome Res.* 2011, 10, 3802–3813

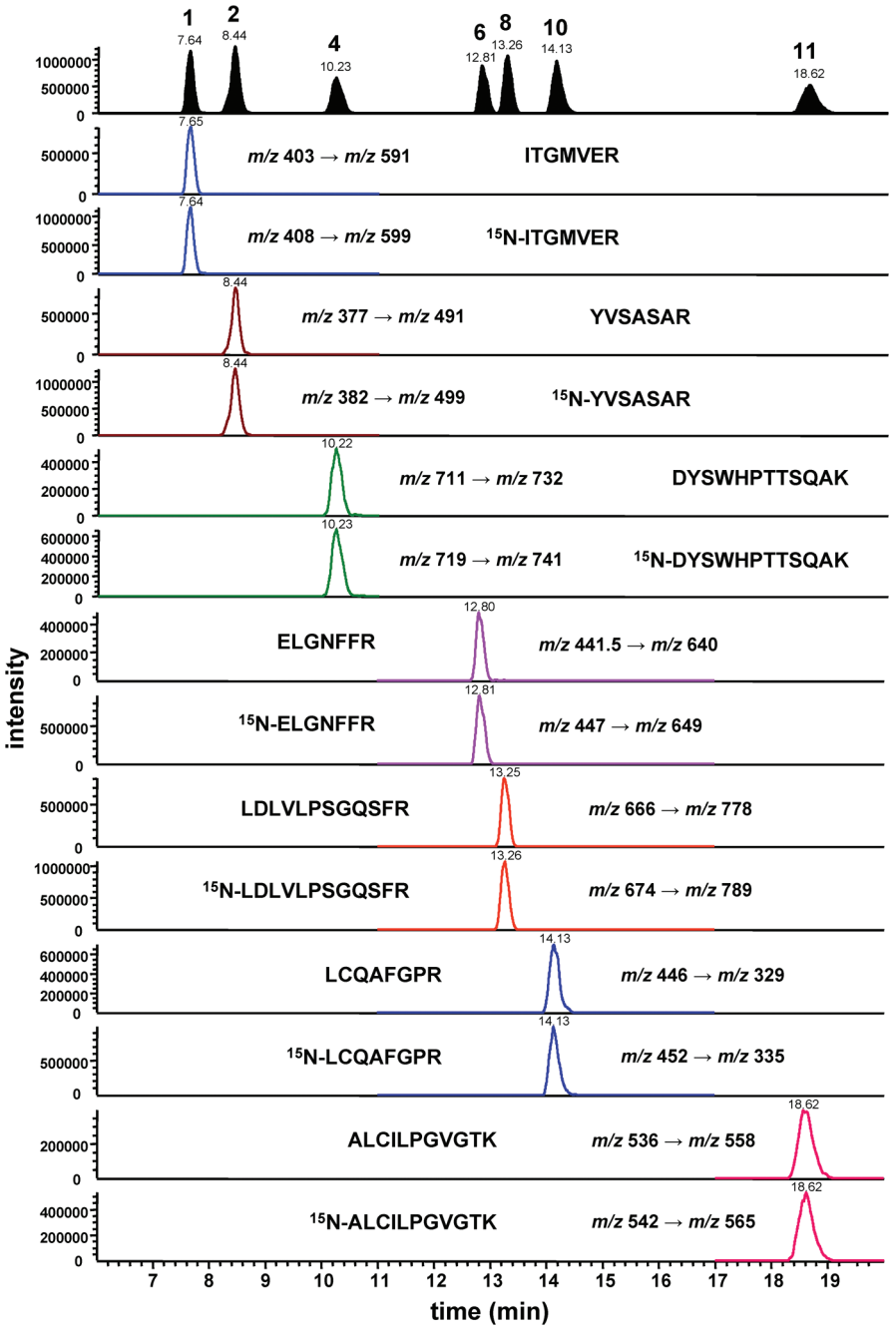

Figure 4. SRM of seven unlabeled peptides and their ^{15}N-labeled analogues from the tryptic digest of a mixture of hOGG1 and ^{15}N-labeled hOGG1. The upper part of the figure illustrates the TIC profiles of all monitored transitions. The peak numbers correspond to those in Table 1 and Figure 1. Peptides and measured transitions are shown.

peptides are given in Table 1. Analysis of the hydrolysate of ^{15}N-labeled hOGG1 yielded an essentially identical TIC profile with 11 analogous peptides as shown in Figure 1B. The monoisotopic masses of the protonated molecular ions (MH^+ ion) and doubly protonated (charged) molecular ions [$(M + 2H)^{2+}$ ion] of the unlabeled and ^{15}N-labeled peptides are also given in Table 1. Using the "MASCOT" search engine (http://www.matrixscience.com) and the 11 identified tryptic peptides, a protein score of 153 was obtained. According to this search engine, protein scores greater than 56 are significant ($p < 0.05$). This means that the 11 tryptic peptides would unequivocally identify this protein. The full-scan spectra of the tryptic peptides were dominated by MH^+ ion and $(M + 2H)^{2+}$ ions. As an example, the mass spectrum taken from the peptide represented by peak 2 in Figure 1A is shown in Figure 2A. This spectrum contains intense MH^+ and $(M + 2H)^{2+}$ ions at m/z 753 and at m/z 377, respectively. Figure 2B illustrates the spectrum of the ^{15}N-labeled analogue of this peptide represented by peak 2 in Figure 1B. As expected, the MH^+ and $(M + 2H)^{2+}$ ions were present at m/z 763 and m/z 382, respectively, because this peptide contains 10 ^{15}N atoms. Typical MNa^+ ions were also observed at m/z 775 and m/z 785. It should be pointed out that we observed no ion at m/z 753 or

dx.doi.org/10.1021/pr200269j |J. Proteome Res. 2011, 10, 3802–3813

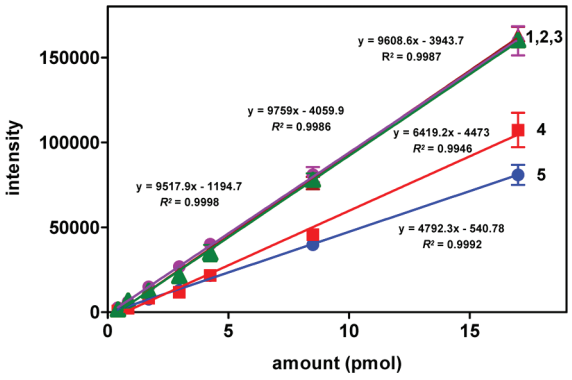

Figure 5. Calibration plots obtained using varying amounts of hOGG1 following trypsin digestion. SRM transitions leading to the most intense ions in the MS/MS spectra of five tryptic peptides were used. (1) ITGMVER, transition m/z 403 → m/z 591; (2) YVSASAR, transition m/z 377 → m/z 491; (3) LDLVLPSGQSFR, transition m/z 666 → m/z 778; (4) DYSWHPTTSQAK, transition m/z 711 → m/z 732; (5) ELGNFFR, transition m/z 441.5 → m/z 640. Each data point represents the mean of three independently measured values. Uncertainties are standard deviations. Results of linear regression analyses are shown. Correlation coefficients (R^2) were >0.99 for all transitions.

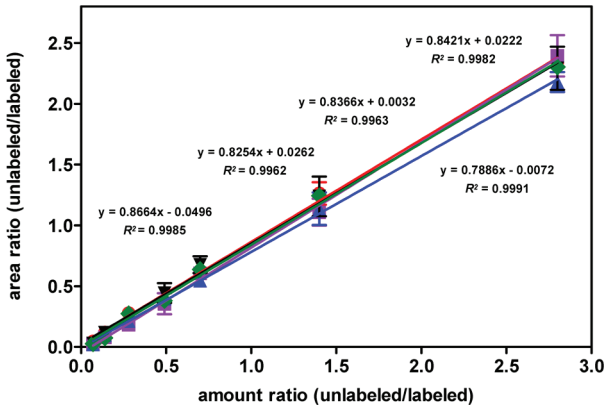

Figure 6. MS/MS response to increasing concentration ratios of tryptic peptides of hOGG1 and their ^{15}N-labeled analogues. Peptides and transitions were as in Figure 5. For ^{15}N-labeled peptides, corresponding transitions were used (see also Figure 4 for transitions). Each data point represents the mean of three independently measured values. Uncertainties are standard deviations. Results of linear regression analyses are shown. Correlation coefficients (R^2) were >0.99 for all transitions.

m/z 377 in Figure 2B, suggesting that the ^{15}N-labeled peptide contained no discernible unlabeled material. The ions at m/z 590 (Figure 2A) and m/z 599 (Figure 2B) represent the y_6-ion of the typical y-ion series, which will be discussed below with the product ion spectra of the peptides. Other examples of the full-scan spectra of the tryptic peptides are illustrated in Figures S1−S3 of the Supporting Information. These spectra and those of the other peptides listed in Table 1 were also dominated by the MH^+ and $(M + 2H)^{2+}$ ions and the ^{15}N-labeled peptides had correct mass shifts according to the number of their ^{15}N atoms. No masses of unlabeled materials were observed in the spectra of all ^{15}N-labeled peptides. Some mass spectra also contained ions of the typical y-ion series. Typically, the $(M + 2H)^{2+}$ ion was more intense than the MH^+ ion in the full-scan mass spectra (data not shown).

Product Ion Spectra of the Tryptic Peptides of hOGG1

Next, we recorded the product ion spectra (MS/MS spectra) of the tryptic peptides using the $(M + 2H)^{2+}$ ions as the precursor ions, because these ions were more intense than MH^+ ions in the full-scan mass spectra. Several experiments were conducted to find out the optimal collision energies yielding the typical fragment ions of each peptide. Optimum collision energies were found to vary from 20 to 32 V. This range is in agreement with that given in the literature for peptides similar in size to those investigated in the present work.[47] We calculated all possible theoretical masses of the typical y- and b-series ions of the identified 11 peptides and their ^{15}N-labeled analogues. These values, which are shown in Tables S1 and S2 of the Supporting Information, were on par with those calculated using the "ProteinProspector" database of the University of California (http://prospector.ucsf.edu/prospector/cgi-bin/msform.cgi?form=msproduct). As an example, Figure 3 illustrates the MS/MS spectrum of LDLVLPSGQSFR (identified as peak 8 in Figure 1A and Table 1). The spectrum was dominated by the y-ion series (Supporting Information Table S1) from the y_4-ion to the y_{11}-ion with different intensities, with the y_7-ion being the most intense ion at m/z 778. The typical b-ion series (Supporting Information Table S2) was represented by the b_2-, b_3-, b_4-, and b_5-ions at m/z 229, 342, 441, and 554, respectively. The ^{15}N-labeled analogue of this peptide yielded a nearly identical MS/MS spectrum with expected mass shifts according to the ^{15}N-content of each fragment ion (Figure 3B). The most prominent y_7-ion appeared at m/z 789. To some extent, the $(M + 2H)^{2+}$ ions were still present in both spectra at m/z 666 and m/z 674.

Several other examples of the MS/MS spectra are given in Figures S4−S6 of the Supporting Information. All ions of the y-ion series from y_1-ion to y_6-ion (Supporting Information Table S1) were observed in the MS/MS spectrum of ITGMVER (represented by peak 1 in Figure 1A) (Supporting Information Figure S4A). The most intense ions were the y_5-ion at m/z 591 and the y_6-ion at m/z 692. The ^{15}N-labeled analogue of this peptide yielded the same ions with masses shifted to higher masses according to the ^{15}N-content of each y-ion (Supporting Information Figure S4B and Table S1). The b-series ions (Supporting Information Table S2) were not prominent with the b_2-ion being the only one observed at m/z 215 or m/z 217. Some ions resulting from loss of NH_3 from y-ions (y-NH_3 ion) were also observed as indicated in the spectra. The $(M + 2H)^{2+}$ ion was not present, indicating the complete fragmentation of the molecule at the collision energy used. The MS/MS spectrum of LCQAFGPR (represented by peak 10 in Figure 1A) was dominated by intense y_3- to y_7-ions (Supporting Information Figure S5A and Table S1). Low intensity y_1- and y_2-ions were also present. Some y-NH_3 ions were observed as indicated in the spectrum. The b_2-, b_3-, b_4-, and b_5-ions (Supporting Information Table S2) with low intensity were found at m/z 217, 345, 416, and 563, respectively. Corresponding ions with expected correct mass shifts were present in the MS/MS spectrum of the ^{15}N-labeled analogue that contains 12 ^{15}N atoms (Supporting Information Figure S5B). The y_6-, y_7-, y_8-, and y_9-ions dominated the MS/MS spectra of ALCILPGVGTK (represented by peak 11 in Figure 1A) and its ^{15}N-labeled analogue (represented by peak 11 in Figure 1B) with the b_2-, b_3-, b_4-, and b_5-ions being present with lower intensity (Supporting Information Figure S6A,B and Tables S1 and S2). Some y-NH_3 ions were observed with low

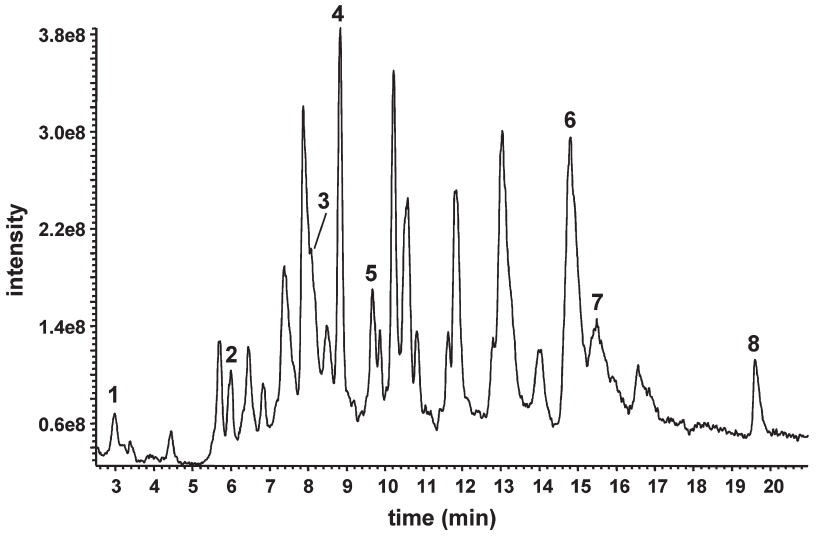

Figure 7. TIC profile of a tryptic digest of Fpg. Identities of the peaks are given in Table 2.

Table 2. Identification of the Peaks in Figure 7[a]

		unlabeled peptide		^{15}N-labeled peptide	
peak	peptide	MH^+	$(M+2H)^{2+}$	MH^+	$(M+2H)^{2+}$
1	ILPEELPPEK	1164.6	582.8	1175.6	588.3
2	SIEQGGTTLK	1033.6	517.3	1045.6	523.3
3	WPVSEEIYR	1178.6	589.8	1191.6	596.3
4	LSDQPVLSVQR	1241.7	621.3	1257.7	629.3
5	AVLLR	571.4	286.2	579.4	290.2
6	VLR	387.3	194.1	393.3	197.1
7	TAIKPWLMDNK	1316.7	658.9	1332.7	666.9
8	FGAWLWTK	1008.5	504.8	1019.5	510.3

[a] Sequences of the tryptic peptides of Fpg and monoisotopic masses (Da) of their MH^+ and $(M + 2H)^{2+}$ ions.

intensity. The mass shifts in the spectrum of ^{15}N-ALCILPGVGTK agreed with the ^{15}N-content of each fragment ion. The MS/MS spectra of the other peptides and their ^{15}N-labeled analogues also contained typical ions of the b-ion and y-ion series. The latter series was more dominant than the former one as in the case of peptides discussed above. Also, the mass shifts due to ^{15}N-labeling were on par with the number of the N atoms in the molecules (data not shown).

Measurement Using Selected-Reaction Monitoring

To validate the method, we analyzed a mixture of hOGG1 and ^{15}N-labeled hOGG1 after trypsin digestion using SRM mode of the MS/MS instrument. This type of analysis is generally used for the identification and quantification of peptides at low concentrations. We monitored the transition of $(M + 2H)^{2+}$ as the precursor ion to the most intense product ion in the MS/MS spectrum of a given peptide during analysis by LC−MS/MS with SRM. $(M + 2H)^{2+}$ ions were used. Figure 4 illustrates ion-current profiles of the transitions of seven tryptic peptides from the mixture of hOGG1 and ^{15}N-hOGG1. The upper part shows the TIC profile of the monitored transitions. Peak numbers correspond to those in Figure 1 and Table 1. As expected, two transition profiles, one of the unlabeled and the other one of the ^{15}N-labeled versions of the same peptide, lined up at the same retention time. Figure 4 clearly shows that a baseline separation of these peptides was achieved and the peak shapes of their transition profiles were excellent for positive identification and accurate quantification of hOGG1.

Analytical Sensitivity of LC−MS/MS for Tryptic Peptides

The analytical sensitivity of the instrument was examined by analyzing tryptic peptides resulting from the proteins. The protein amounts ranged from 5 to 100 fmol injected on-column. The limit of detection (LOD) was approximately 10 fmol with a signal-to-noise ratio (S/N) of 3. The limit of quantification (LOQ) was approximately 30 fmol with an S/N of 10 (data not shown).

Calibration Plots

The linear calibration range of the response of the MS/MS instrument for the peptide analytes was assessed using SRM with proper transitions and amount of the peptides ranging from 0.42 pmol/analyte to 17 pmol/analyte injected on-column. A linear response was observed. As examples, Figure 5 illustrates the calibration plots of five peptides. The responses of three peptides were nearly identical, whereas the other two peptides gave somewhat lower response for the ions monitored. A calibration plot was also generated using peak area ratios versus concentration ratios of the unlabeled and labeled forms of the same peptide. A linear response was obtained within a concentration ratio ranging from 0.25 to 8.0 (Figure 6).

Analysis of *E. coli* Fpg

Figure 7 illustrates the TIC profile of the trypsin hydrolysate of Fpg. The trypsin hydrolysate of ^{15}N-labeled Fpg provided an essentially identical TIC profile (not shown). The full-scan mass spectra of the tryptic peptides were recorded. Eight peptides were identified, matching the theoretical peptide fragments expected from the trypsin digestion of Fpg (Table 2). Using the "MASCOT" search engine and the eight identified peptides, a protein score of 118 ($p < 0.05$) was obtained, indicating that these peptides would unequivocally identify Fpg. The full-scan mass spectra of the tryptic peptides of Fpg contained intense MH^+ ion and $(M + 2H)^{2+}$ ions. As an example, Figure 8A and B illustrates the full-scan mass spectra of LSDQPVLSVQR

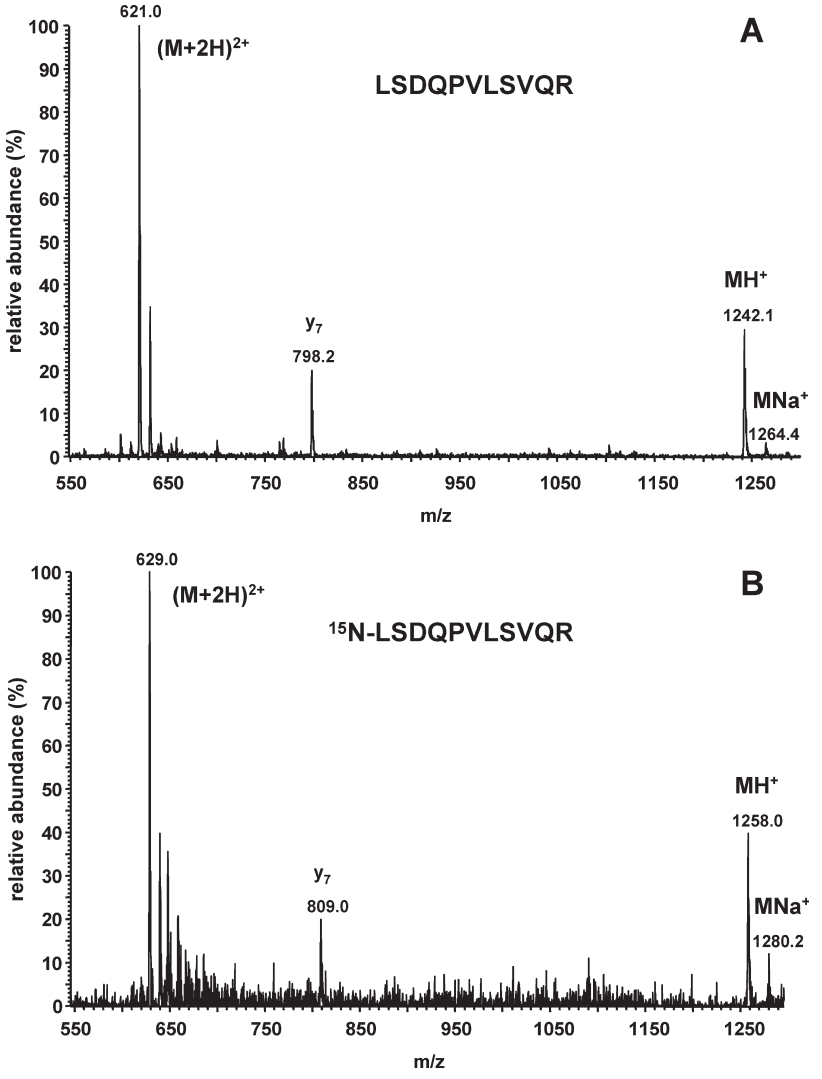

Figure 8. Full-scan mass spectra of (A) LSDQPVLSVQR (peak 4 in Figure 7) and (B) ^{15}N-LSDQPVLSVQR.

(represented by peak 4 in Figure 7) and ^{15}N-LSDQPVLSVQR, respectively. Low intensity MNa^+ ions were also present.

Product Ion Spectra of the Tryptic Peptides of Fpg

The MS/MS spectra were recorded using the $(M + 2H)^{2+}$ ion as the precursor ion for each of the identified eight tryptic peptides of Fpg. Collision energies used were similar to those used for the tryptic peptides of hOGG1. We calculated theoretical masses of the typical y- and b-series ions of the identified tryptic peptides and their ^{15}N-labeled analogues (Supporting Information Tables S3 and S4). They were identical to those obtained using the aforementioned "ProteinProspector" database. As an example, the MS/MS spectra of LDLVLPSGQSFR and ^{15}N-LDLVLPSGQSFR are illustrated in Figure 9. These spectra were dominated by the y-ion series from the y_3-ion to the y_{10}-ion with different intensities, with the y_7-ion being the most intense ion at m/z 798 or m/z 809 (fragmentation patterns not shown due to space limitation). In general, intensities of the b-series ions were of low intensity. Similarly, the MS/MS spectra of the other tryptic peptides of Fpg and their ^{15}N-labeled analogues yielded the typical y- and b-series ions (data not shown).

Measurement Using Selected-Reaction Monitoring and Calibration Plots

For validation of the method, unlabeled Fpg and ^{15}N-labeled Fpg were mixed, hydrolyzed with trypsin, and analyzed by LC−MS/MS with SRM. The transition of the $(M + 2H)^{2+}$ ion to the most intense product ion in the MS/MS spectra was monitored for each peptide. Baseline separation of the peptides was obtained with transition profiles of the unlabeled and labeled versions of the same peptide lined up at the same retention time. As in the case of hOGG1, the profiles showed their excellent suitability for quantification of the corresponding peptides (data not shown). Linear calibration plots were obtained with tryptic peptides of Fpg as well. The ranges of peptide amounts and ratio of unlabeled/labeled peptides were similar to those resulting from hOGG1 (data not shown).

■ DISCUSSION

We developed mass spectrometric assays for the positive identification and accurate quantification of two major mammalian and bacterial DNA repair proteins, hOGG1 and *E.coli* Fpg. We used fully ^{15}N-labeled analogues of these proteins as internal standards for quantification. This approach is different from

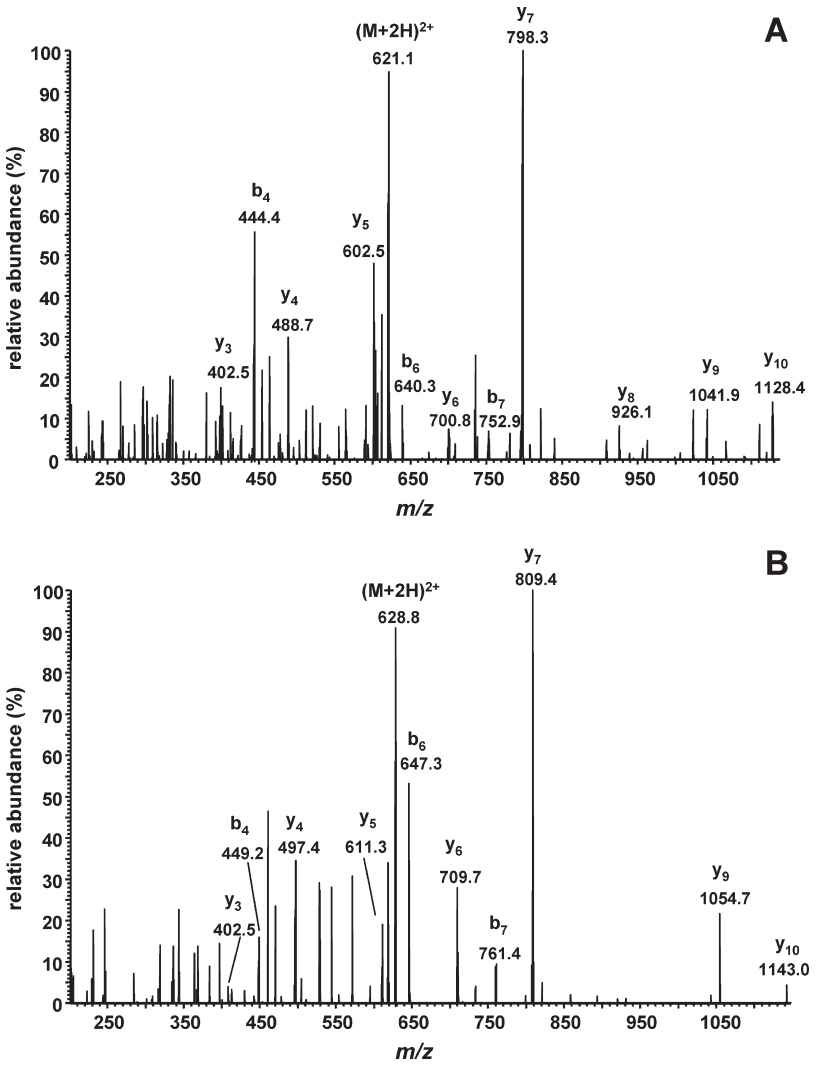

Figure 9. MS/MS spectra of (A) LSDQPVLSVQR (peak 4 in Figure 7) and (B) ^{15}N-LSDQPVLSVQR, respectively. Fragmentation pathways leading to the b- and y-series ions are not shown because of the limited space in the figure.

those that use isotopically labeled tryptic peptides as internal standards. Trypsin digestion can often be inefficient depending on the protein and amide bond conditions, leading to incomplete yields of tryptic peptides and consequently to potential measurement bias. Therefore, the use of the fully ^{15}N-labeled analogue of an analyte protein as an internal standard is essential for accurate mass spectrometric measurements. Moreover, the advantage of the labeled protein over a labeled tryptic peptide is that it will have identical chemical and physical properties as the analyte protein and can be added to a sample at the earliest step of sample preparation. This would compensate for eventual losses that may occur during all stages of analysis. A labeled tryptic peptide would not meet these requirements. The use of labeled analogues of analyte proteins would especially be of utmost importance in the case of the isolation of proteins by two-dimensional gel electrophoresis and their "in-gel digestion" prior to analysis by LC−MS/MS.

In the case of both hOGG1 and Fpg, we observed numerous tryptic peptides that were well separated and provided mass spectra with intense MH^+ and $(M + 2H)^{2+}$ ions. With the identified tryptic peptides, statistically significant high protein scores were obtained, meaning that those peptides would unequivocally identify hOGG1 or Fpg. Using $(M + 2H)^{2+}$ as the precursor ions, MS/MS spectra yielded typical ions of the b- and y-ion series, expected from the fragmentation of the peptides. Trypsin digestion of ^{15}N-labeled proteins led to tryptic peptides identical to those of their unlabeled counterparts with shifts in masses of the observed ions according to the ^{15}N-content of each peptide. We observed no discernible unlabeled material in ^{15}N-labeled proteins. This meets an absolutely essential requirement for an ideal stable isotope-labeled internal standard. We also demonstrated the use of SRM for identification and quantification. Our method using ^{15}N-labeled hOGG1 as the internal standard will also be useful for the measurement of the other main isoform β-hOGG1 located to the mitochondrion. This is because α-hOGG1 and β-hOGG1 have an identical sequence up to 316 amino acids at the N-terminus albeit different total lengths and molecular masses.[45] Trypsin digestion would yield 30 identical tryptic peptides from both proteins. The 11 peptides identified in this work are among those 30 peptides.

There are polymorphic variants and mutants of hOGG1 that have been discovered in human tissues. The measurement of such proteins may contribute to understanding of their role in disease processes. However, this approach will be challenging in

that each of these variants and mutants will have to be overexpressed and isolated in pure form to first understand their liquid chromatographic and mass spectrometric behaviors, and the mass spectra and fragmentation patterns of their tryptic peptides. Moreover, ^{15}N-labeled analogues of each of these proteins must be overproduced and purified to serve as suitable internal standards for accurate quantification as outlined in this paper for the wild-type (wt-) hOGG1. The protein expression must also be optimized for each protein. The best known example among hOGG1 variants is hOGG1-Cys^{326} which results from a genetic polymorphism at codon 326 (Ser326Cys). This variant has been found frequently in human populations and several cancers.[15,22,25,48−50] It possesses the same specificity as wt-OGG1 for the excision of FapyGua and 8-OH-Gua from DNA, albeit with about 2-fold reduced activity.[26] Since hOGG1-Cys^{326} has one amino acid replacement only, all the tryptic peptides with one exception, namely, QSR, would have the identical sequence to those of wt-hOGG1. This means that the ^{15}N-labeled hOGG1 as used in this work may also serve as suitable internal standard for hOGG1-Cys^{326}. Moreover, even if two-dimensional gel electrophoresis is used prior to LC−MS/MS, hOGG1-Cys^{326} is not expected to migrate any differently from hOGG1. Two other mutant forms of wt-hOGG1, namely, hOGG1-His^{154} and hOGG1-Gln,[46] have been found in a human gastric cancer cell line and human kidney tumors, respectively.[17,49] These mutants had significantly reduced activity for FapyGua and 8-OH-Gua when compared to wt-OGG1.[27] Both mutations are due to the replacement of Arg, modifying one tryptic peptide, which is one of the 11 tryptic peptides of wt-OGG1 identified in the present work. Therefore, ^{15}N-labeled wt-OGG1 would still be a suitable internal standard for these mutant proteins as well because the remaining 10 tryptic peptides would be sufficient for accurate quantification. However, migration properties of these proteins are not known when two-dimensional gel electrophoresis is used. Other variants or mutants of OGG1 yet to be discovered may also be challenging, perhaps even more so, for mass spectrometric measurements. Each protein must be dealt with separately, isolated and purified, and must go through vigorous investigation as done in the present work. The mutations and migration properties of each variant or mutant of OGG1 will determine whether new stable isotope-labeled internal standards are needed, or whether ^{15}N-labeled wt-OGG1, as described here and elsewhere,[41] would be a suitable internal standard.

Genetic instability caused by DNA damage may alter expression of proteins involved in DNA repair pathways, chromosomal stability among others.[10] Altered DNA repair gene expression may affect DNA repair status of tumors. DNA repair pathways are promising drug targets for cancer treatment, and DNA repair inhibitors are being developed to increase the efficacy of therapy.[11,13] Moreover, accumulated evidence points to DNA repair proteins as important early detection, prognostic, and therapeutic factors in cancer and perhaps in other diseases. Thus, the accurate measurement of DNA repair proteins in vivo may be essential for their use as disease biomarkers. hOGG1 is one of the major DNA repair enzymes involved in the first step of multistep BER of oxidatively induced DNA damage. The accurate measurement of this enzyme in living tissues will be important for understanding of DNA repair of this type of DNA damage and its relation to disease processes including carcinogenesis.

CONCLUSIONS

We believe that the methodology developed in this work with the use of LC−MS/MS with isotope-dilution using fully labeled proteins as internal standards will be highly suitable for the positive identification and accurate quantification of hOGG1 and Fpg in vivo. This methodology is likely to be applicable for the measurement of other DNA repair proteins as long as stable isotope-labeled whole proteins can be produced and purified to be used as internal standards. The measurement of DNA repair proteins will be of fundamental importance for understanding of their role in disease processes, for development of DNA repair inhibitors, and for their use as biomarkers for early detection, prognosis, and efficacy of therapy.

ASSOCIATED CONTENT

Supporting Information

Figures S1−S6 and Tables S1−S4. This material is available free of charge via the Internet at http://pubs.acs.org.

AUTHOR INFORMATION

Corresponding Author

*Mailing address: 100 Bureau Drive, MS8311, Gaithersburg, MD 20899, USA. Telephone: 301-975-2581. Fax: 301-975-8505. E-mail: miral@nist.gov.

ACKNOWLEDGMENT

Certain commercial equipment or materials are identified in this paper in order to specify adequately the experimental procedure. Such identification does not imply recommendation or endorsement by the National Institute of Standards and Technology, nor does it imply that the materials or equipment identified are necessarily the best available for the purpose.

REFERENCES

(1) Evans, M. D.; Dizdaroglu, M.; Cooke, M. S. Oxidative DNA damage and disease: induction, repair and significance. *Mutat. Res.* **2004**, *567*, 1–61.

(2) Friedberg, E. C.; Walker, G. C.; Siede, W.; Wood, R. D.; Schultz, R. A.; Ellenberger, T. *DNA Repair and Mutagenesis*, second ed.; ASM Press: Washington, D.C., 2005.

(3) Hoeijmakers, J. H. Genome maintenance mechanisms for preventing cancer. *Nature* **2001**, *411*, 366–374.

(4) Cheng, L.; Eicher, S. A.; Guo, Z. Z.; Hong, W. K.; Spitz, M. R.; Wei, Q. Y. Reduced DNA repair capacity in head and neck cancer patients. *Cancer Epidemiol., Biomarkers Prev.* **1998**, *7*, 465–468.

(5) Berwick, M.; Vineis, P. Markers of DNA repair and susceptibility to cancer in humans: an epidemiologic review. *J. Natl. Cancer Inst.* **2000**, *92*, 874–897.

(6) Cheng, L.; Spitz, M. R.; Hong, W. K.; Wei, Q. Reduced expression levels of nucleotide excision repair genes in lung cancer: a case-control analysis. *Carcinogenesis* **2000**, *21*, 1527–1530.

(7) Lippman, S. M.; Spitz, M. R. Lung cancer chemoprevention: an integrated approach. *J. Clin. Oncol.* **2001**, *19*, 74S–82S.

(8) Goode, E. L.; Ulrich, C. M.; Potter, J. D. Polymorphisms in DNA repair genes and associations with cancer risk. *Cancer Epidemiol., Biomarkers Prev.* **2002**, *11*, 1513–1530.

(9) Morimoto, H.; Tsukada, J.; Kominato, Y.; Tanaka, Y. Reduced expression of human mismatch repair genes in adult T-cell leukemia. *Am. J. Hematol.* **2005**, *78*, 100–107.

(10) Beckman, R. A.; Loeb, L. A. Genetic instability in cancer: theory and experiment. *Semin. Cancer Biol.* **2005**, *15*, 423–435.

(11) Madhusudan, S.; Middleton, M. R. The emerging role of DNA repair proteins as predictive, prognostic and therapeutic targets in cancer. *Cancer Treat. Rev.* **2005**, *31*, 603–617.

(12) Liu, R.; Yin, L. H.; Pu, Y. P. Reduced expression of human DNA repair genes in esophageal squamous-cell carcinoma in china. *J. Toxicol. Environ. Health, Part A* **2007**, *70*, 956–963.

(13) Helleday, T.; Petermann, E.; Lundin, C.; Hodgson, B.; Sharma, R. A. DNA repair pathways as targets for cancer therapy. *Nat. Rev. Cancer* **2008**, *8*, 193–204.

(14) Loeb, L. A. Mutator phenotype in cancer: origin and consequences. *Semin. Cancer Biol.* **2010**, *20*, 279–280.

(15) Chevillard, S.; Radicella, J. P.; Levalois, C.; Lebeau, J.; Poupon, M. F.; Oudard, S.; Dutrillaux, B.; Boiteux, S. Mutations in *OGG1*, a gene involved in the repair of oxidative DNA damage, are found in human lung and kidney tumours. *Oncogene* **1998**, *16*, 3083–3086.

(16) Sugimura, H.; Kohno, T.; Wakai, K.; Nagura, K.; Genka, K.; Igarashi, H.; Morris, B. J.; Baba, S.; Ohno, Y.; Gao, C.; Li, Z.; Wang, J.; Takezaki, T.; Tajima, K.; Varga, T.; Sawaguchi, T.; Lum, J. K.; Martinson, J. J.; Tsugane, S.; Iwamasa, T.; Shinmura, K.; Yokota, J. hOGG1 Ser326Cys polymorphism and lung cancer susceptibility. *Cancer Epidemiol., Biomarkers Prev.* **1999**, *8*, 669–674.

(17) Audebert, M.; Chevillard, S.; Levalois, C.; Gyapay, G.; Vieillefond, A.; Klijanienko, J.; Vielh, P.; El Naggar, A. K.; Oudard, S.; Boiteux, S.; Radicella, J. P. Alterations of the DNA repair gene OGG1 in human clear cell carcinomas of the kidney. *Cancer Res.* **2000**, *60*, 4740–4744.

(18) Elahi, A.; Zheng, Z.; Park, J.; Eyring, K.; McCaffrey, T.; Lazarus, P. The human OGG1 DNA repair enzyme and its association with orolaryngeal cancer risk. *Carcinogenesis* **2002**, *23*, 1229–1234.

(19) Chen, L.; Elahi, A.; Pow-Sang, J.; Lazarus, P.; Park, J. Association between polymorphism of human oxoguanine glycosylase 1 and risk of prostate cancer. *J. Urol.* **2003**, *170*, 2471–2474.

(20) Weiss, J. M.; Goode, E. L.; Ladiges, W. C.; Ulrich, C. M. Polymorphic variation in hOGG1 and risk of cancer: a review of the functional and epidemiologic literature. *Mol. Carcinog.* **2005**, *42*, 127–141.

(21) Hung, R. J.; Hall, J.; Brennan, P.; Boffetta, P. Genetic polymorphisms in the base excision repair pathway and cancer risk: a HuGE review. *Am. J. Epidemiol.* **2005**, *162*, 925–942.

(22) Kohno, T.; Kunitoh, H.; Toyama, K.; Yamamoto, S.; Kuchiba, A.; Saito, D.; Yanagitani, N.; Ishihara, S.; Saito, R.; Yokota, J. Association of the OGG1-Ser326Cys polymorphism with lung adenocarcinoma risk. *Cancer Sci.* **2006**, *97*, 724–728.

(23) Goto, M.; Shinmura, K.; Yamada, H.; Tsuneyoshi, T.; Sugimura, H. OGG1, MYH and MTH1 gene variants identified in gastric cancer patients exhibiting both 8-hydroxy-2′-deoxyguanosine accumulation and low inflammatory cell infiltration in their gastric mucosa. *J. Genet.* **2008**, *87*, 181–186.

(24) Farinati, F.; Cardin, R.; Bortolami, M.; Nitti, D.; Basso, D.; de, B. M.; Cassaro, M.; Sergio, A.; Rugge, M. Oxidative DNA damage in gastric cancer: CagA status and OGG1 gene polymorphism. *Int. J. Cancer* **2008**, *123*, 51–55.

(25) Arizono, K.; Osada, Y.; Kuroda, Y. DNA repair gene hOGG1 codon 326 and XRCC1 codon 399 polymorphisms and bladder cancer risk in a Japanese population. *Jpn. J. Clin. Oncol.* **2008**, *38*, 186–191.

(26) Dherin, C.; Radicella, J. P.; Dizdaroglu, M.; Boiteux, S. Excision of oxidatively damaged DNA bases by the human alpha-hOgg1 protein and the polymorphic alpha-hOgg1(Ser326Cys) protein which is frequently found in human populations. *Nucleic Acids Res.* **1999**, *27*, 4001–4007.

(27) Audebert, M.; Radicella, J. P.; Dizdaroglu, M. Effect of single mutations in the OGG1 gene found in human tumors on the substrate specificity of the ogg1 protein. *Nucleic Acids Res.* **2000**, *28*, 2672–2678.

(28) Sidorenko, V. S.; Grollman, A. P.; Jaruga, P.; Dizdaroglu, M.; Zharkov, D. O. Substrate specificity and excision kinetics of natural polymorphic variants and phosphomimetic mutants of human 8-oxoguanine-DNA glycosylase. *FEBS J.* **2009**, *276*, 5149–5162.

(29) Bosken, C. H.; Wei, Q.; Amos, C. I.; Spitz, M. R. An analysis of DNA repair as a determinant of survival in patients with non-small-cell lung cancer. *J. Natl. Cancer Inst.* **2002**, *94*, 1091–1099.

(30) Lord, R. V.; Brabender, J.; Gandara, D.; Alberola, V.; Camps, C.; Domine, M.; Cardenal, F.; Sanchez, J. M.; Gumerlock, P. H.; Taron, M.; Sanchez, J. J.; Danenberg, K. D.; Danenberg, P. V.; Rosell, R. Low ERCC1 expression correlates with prolonged survival after cisplatin plus gemcitabine chemotherapy in non-small cell lung cancer. *Clin. Cancer Res.* **2002**, *8*, 2286–2291.

(31) Rosell, R.; Taron, M.; Barnadas, A.; Scagliotti, G.; Sarries, C.; Roig, B. Nucleotide excision repair pathways involved in Cisplatin resistance in non-small-cell lung cancer. *Cancer Control* **2003**, *10*, 297–305.

(32) Gackowski, D.; Speina, E.; Zielinska, M.; Kowalewski, J.; Rozalski, R.; Siomek, A.; Paciorek, T.; Tudek, B.; Olinski, R. Products of oxidative DNA damage and repair as possible biomarkers of susceptibility to lung cancer. *Cancer Res.* **2003**, *63*, 4899–4902.

(33) Paz-Elizur, T.; Krupsky, M.; Blumenstein, S.; Elinger, D.; Schechtman, E.; Livneh, Z. DNA repair activity for oxidative damage and risk of lung cancer. *J. Natl. Cancer Inst.* **2003**, *95*, 1312–1319.

(34) Paz-Elizur, T.; Ben-Yosef, R.; Elinger, D.; Vexler, A.; Krupsky, M.; Berrebi, A.; Shani, A.; Schechtman, E.; Freedman, L.; Livneh, Z. Reduced repair of the oxidative 8-oxoguanine DNA damage and risk of head and neck cancer. *Cancer Res.* **2006**, *66*, 11683–11689.

(35) Paz-Elizur, T.; Elinger, D.; Leitner-Dagan, Y.; Blumenstein, S.; Krupsky, M.; Berrebi, A.; Schechtman, E.; Livneh, Z. Development of an enzymatic DNA repair assay for molecular epidemiology studies: distribution of OGG activity in healthy individuals. *DNA Repair* **2007**, *6*, 45–60.

(36) Tudek, B. Base excision repair modulation as a risk factor for human cancers. *Mol. Aspects Med.* **2007**, *28*, 258–275.

(37) El-Zein, R. A.; Monroy, C. M.; Cortes, A.; Spitz, M. R.; Greisinger, A.; Etzel, C. J. Rapid method for determination of DNA repair capacity in human peripheral blood lymphocytes amongst smokers. *BMC Cancer* **2010**, *10*, 439.

(38) Sudprasert, W.; Navasumrit, P.; Ruchirawat, M. Effects of low-dose gamma radiation on DNA damage, chromosomal aberration and expression of repair genes in human blood cells. *Int. J. Hyg. Environ. Health* **2006**, *209*, 503–511.

(39) Mambo, E.; Chatterjee, A.; de Souza-Pinto, N. C.; Mayard, S.; Hogue, B. A.; Hoque, M. O.; Dizdaroglu, M.; Bohr, V. A.; Sidransky, D. Oxidized guanine lesions and hOgg1 activity in lung cancer. *Oncogene* **2005**, *24*, 4496–4508.

(40) Obtulowicz, T.; Swoboda, M.; Speina, E.; Gackowski, D.; Rozalski, R.; Siomek, A.; Janik, J.; Janowska, B.; Ciesla, J. M.; Jawien, A.; Banaszkiewicz, Z.; Guz, J.; Dziaman, T.; Szpila, A.; Olinski, R.; Tudek, B. Oxidative stress and 8-oxoguanine repair are enhanced in colon adenoma and carcinoma patients. *Mutagenesis* **2010**, *25*, 463–471.

(41) Reddy, P. T.; Jaruga, P.; Nelson, B. C.; Lowenthal, M.; Dizdaroglu, M. Stable isotope-labeling of DNA repair proteins, and their purification and characterization. *Protein Expression Purif.* **2011**, *78*, 94–101.

(42) Monden, Y.; Arai, T.; Asano, M.; Ohtsuka, E.; Aburatani, H.; Nishimura, S. Human MMH (OGG1) type 1a protein is a major enzyme for repair of 8-hydroxyguanine lesions in human cells. *Biochem. Biophys. Res. Commun.* **1999**, *258*, 605–610.

(43) Takao, M.; Aburatani, H.; Kobayashi, K.; Yasui, A. Mitochondrial targeting of human DNA glycosylases for repair of oxidative DNA damage. *Nucleic Acids Res.* **1998**, *26*, 2917–2922.

(44) Nishioka, K.; Ohtsubo, T.; Oda, H.; Fujiwara, T.; Kang, D.; Sugimachi, K.; Nakabeppu, Y. Expression and differential intracellular localization of two major forms of human 8-oxoguanine DNA glycosylase encoded by alternatively spliced OGG1 mRNAs. *Mol. Biol. Cell* **1999**, *10*, 1637–1652.

(45) Boiteux, S.; Radicella, J. P. Base excision repair of 8-hydroxyguanine protects DNA from endogenous oxidative stress. *Biochimie* **1999**, *81*, 59–67.

(46) Eidhammer, I.; Flikka, K.; Martens, L.; Mikalsen, S.-O. *Computational Methods for Mass Spectrometric Proteomics*; John Wiley & Sons, Ltd.: West Sussex, England, 2007.

(47) Kinter, M.; Sherman, N. E. *Protein Sequencing and Identification Using Tandem Mass Spectrometry*; Wiley-Interscience: New York, 2000.

(48) Kohno, T.; Shinmura, K.; Tosaka, M.; Tani, M.; Kim, S. R.; Sugimura, H.; Nohmi, T.; Kasai, H.; Yokota, J. Genetic polymorphisms and alternative splicing of the *hOGG1* gene, that is involved in the repair of 8-hydroxyguanine in damaged DNA. *Oncogene* **1998**, *16*, 3219–3225.

(49) Shinmura, K.; Kohno, T.; Kasai, H.; Koda, K.; Sugimura, H.; Yokota, J. Infrequent mutations of the hOGG1 gene, that is involved in the excision of 8-hydroxyguanine in damaged DNA, in human gastric cancer. *Jpn. J. Cancer Res.* **1998**, *89*, 825–828.

(50) Hansen, R.; Saebo, M.; Skjelbred, C. F.; Nexo, B. A.; Hagen, P. C.; Bock, G.; Bowitz, L., I; Johnson, E.; Aase, S.; Hansteen, I. L.; Vogel, U.; Kure, E. H. GPX Pro198Leu and OGG1 Ser326Cys polymorphisms and risk of development of colorectal adenomas and colorectal cancer. *Cancer Lett.* **2005**, *229*, 85–91.